Properties of Dianionic Oxyphosphorane Intermediates: Implication to the Reaction Profile for Base-Catalyzed RNA Hydrolysis

Kazunari Taira,*[,†,‡] Tadafumi Uchimaru,*[,†,§] Joey W. Storer,[§,⊥] Ari Yliniemela,[§,∥] Masami Uebayasi,[†,‡] and Kazutoshi Tanabe[†,§]

National Institute of Bioscience and Human Technology, and National Institute of Materials and Chemical Research, Agency of Industrial Science & Technology, MITI, Tsukuba Science City 305, Japan

Received August 17, 1992 (Revised Manuscript Received February 24, 1993)

From calculations of a model reaction scheme for base-catalyzed RNA hydrolysis (which also represents the base-catalyzed methanolysis of ethylene phosphate monoanion in reverse), a pentacoordinate dianionic intermediate **2a** (Storer et al. *J. Am. Chem. Soc.* **1991**, *113*, 5216–5219) as well as two transition states, *TS1* and *TS2*, to the intermediate have been located by ab initio calculations at the 3-21G* level. However, the intermediate, which has a well depth on the order of k_BT, is unlikely to be kinetically significant. The endocyclic P–O(2′) bond is found to be much weaker than the exocyclic P–O(5′) bond. In agreement with this finding, calculations on **2a** at the 6-31+G* level abolishes *TS1* and the pentacoordinate intermediate, leaving only *TS2* as the sole transition state. Thus, for all the cases examined, the rate-limiting transition-state structure is *TS2* which has an extended P–O(5′) breaking bond. These results and the mode of cleavage of a simpler compound **3b** are in accord with stereoelectronic predictions (see text for the definition). Moreover, solvation appears to stabilize the pentacoordinate intermediate. In the gas phase, the simplest oxyphosphorane **3b** has the least tendency to form a pentacoordinate intermediate. However, **3b** does form a pentacoordinate intermediate when it is solvated with six water molecules. These results support the hypothesis that phosphoryl-transfer reactions take place via pentacoordinate intermediates not only in acidic but also in basic media.

Introduction

The nature of the nucleotide phosphate backbone is a topic of much current interest. The potential energy surface for the base-catalyzed hydrolysis of the RNA phosphate backbone is therefore a predominant issue in understanding the hydrolyzing mechanism and its relation to the inherent stability of RNA. Recently, Karplus' group and ours initiated ab initio studies on dianionic cyclic oxyphosphoranes, **2a**[1] and **2b**[2] as model compounds of RNA hydrolysis intermediate **1** (see Figure 1 for structural information). Further ab initio calculations were carried out on the acyclic counterparts as well, such as **3a**,[3] **3b**,[4] and **3c**.[5] Depending on the nature (molecular size) of the dianionic pentacoordinate species, they either exist or do not exist as stable intermediates. For example, in contrast to **2b** and **3b**, both **3a** and **3c** exist as marginally stable intermediates at the 3-21G* and 3-21+G* levels. The energy diagrams for the acyclic systems were also analyzed: because of the greater conformational freedom of the acyclic compounds, the gas-phase potential surface showed that the equatorial bond always rotates to a conformation where the lone-pair electrons of the equatorial oxygen are trans antiperiplanar to either the axial nucleophile or leaving group.[3-5] Thus, the lowest energy pathway in the gas phase could in principle be rationalized by the stereoelectronic effect,[6-8] although the long-believed $n_{O3}-\sigma^*_{P-O(axial)}$ orbital interactions do not appear to be the sole cause of the stereoelectronic effect.[9-12]

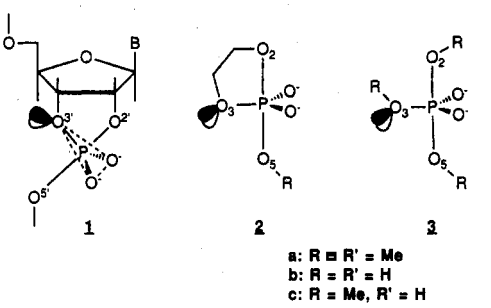

Figure 1. Cyclic and acyclic pentacoordinate oxyphosphoranes. 1: pentacoordinate intermediate in the base-catalyzed hydrolysis of RNA. 2 and 3: cyclic and acyclic model compounds for dianionic pentacoordinate oxyphosphorane species (the lone pair orbitals on the equatorial $O_{(3)}$ oxygen atom are located in the antiperiplanar regions relative to the axial $P-O_{(2)}$ bond, which are dipicted only for the purpose of visualization).

* To whom correspondence should be addressed.

† Before consolidation, which took place on January 1, 1993, K.T. and M.U. belonged to the ‡Fermentation Research Institute and T.U. and K.T. belonged to the §National Chemical Laboratory for Industry.

⊥ On leave from the Department of Chemistry and Biochemistry, University of California, Los Angeles, CA 90024-1569. J.W.S. conducted a portion of this work as a participant in the 1990 Summer Institute in Japan for U.S. Graduate Students in Science and Engineering, supported by the National Science Foundation and the Science and Technology Agency of Japan.

∥ On leave from the Technical Research Centre of Finland, Chemical Laboratory, P.O. Box 204, SF-02151, Finland. A.Y. participated in this study while he was a visting researcher at the National Chemical Laboratory for Industry.

(1) (a) Taira, K.; Uebayasi, M.; Maeda, H.; Furukawa, K. *Protein Eng.* **1990**, *3*, 691–701. (b) Storer, J. W.; Uchimaru, T.; Tanabe, K.; Uebayasi, M.; Nishikawa, S.; Taira, K. *J. Am. Chem. Soc.* **1991**, *113*, 5216–5219.

(2) Lim, C.; Karplus, M. *J. Am. Chem. Soc.* **1990**, *112*, 5872–5873.

(3) Uchimaru, T.; Tanabe, K.; Nishikawa, S.; Taira, K. *J. Am. Chem. Soc.* **1991**, *113*, 4351–4353.

(4) Taira, K.; Uchimaru, T.; Tanabe, K.; Uebayasi, M.; Nishikawa, S. *Nucleic Acids Res.* **1991**, *19*, 2747–2753.

(5) Dejaegere, A.; Lim, C.; Karplus, M. *J. Am. Chem. Soc.* **1991**, *113*, 4353–4355.

(6) (a) Gorenstein, D. G. *Chem. Rev.* **1987**, *87*, 1047–1077. (b) Gorenstein, D. G.; Luxon, B. A.; Findlay, J. B. *J. Am. Chem. Soc.* **1977**, *99*, 8048–8049.

(7) Deslongchamps, P. *Stereoelectronic Effects in Organic Chemistry*; Pergamon Press: New York, 1983.

(8) Kirby, A. J. *The Anomeric Effects and Related Stereoelectronic Effects at Oxygen*: Springer-Verlag: Berlin, 1983.

(9) Sinnott, M. L. In *Enzyme Mechanisms*; Page, M. I., Williams, A., Eds.; Royal Society of Chemistry: London, 1987; p 259.

0022-3263/93/1958-3009$04.00/0

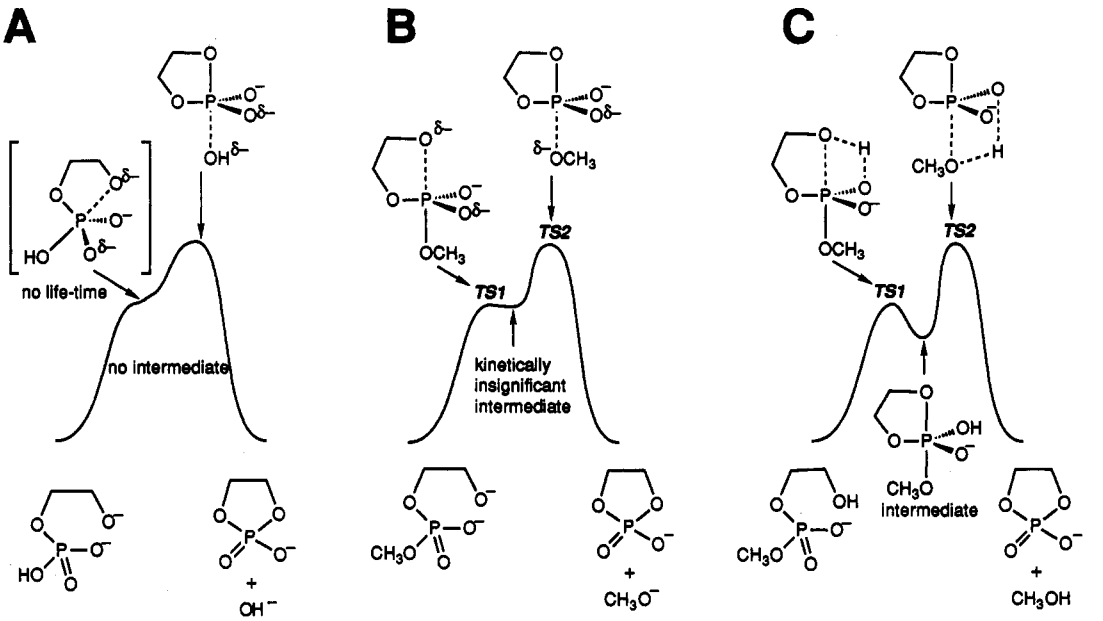

Figure 2. Schematic diagrams showing lifetimes of oxyphosphoranes. Lim and Karplus' dianionic oxyphosphorane (**2b**) does not exist as an intermediate (A).[2] On the other hand, monoanionic oxyphosphorane (**2a**) is definitely intermediate (C).[13] The dianionic oxyphosphorane of this study (B) falls just between these two cases (A and C), and it is not a real intermediate. It is to be noted that in all cases examined the rate-limiting transition-state structures mainly possess P–O(5′) bond-breaking character.

We now analyze a cyclic system in which the above-mentioned rotation of the equatorial bond is prohibited by the cyclic ring formation during the hydrolysis. Here, we report the complete reaction energy surface for $^{-}O(CH_2)_2OP(OCH_3)O_2^{-} \rightarrow (CH_2O)_2PO_2^{-} + OCH_3^{-}$ at the 3-21G* level (Figure 4), representing the attack of an RNA fragment by 2′-alkoxide followed by the expulsion of 5′-alkoxide, i.e., the base-catalyzed RNA hydrolysis via the pentacoordinate intermediate **1** (which also represents the base-catalyzed methanolysis of ethylene phosphate monoanion in reverse).[1] The present energy profile is different from those of the acyclic system: in contrast to the previously reported studies of acyclic counterparts **3a**[3] and **3c**[5], the stereoelectronically unfavorable transition state *TS2* does exist in the case of **1** and **2** because of the unique cyclic nature of the intermediate.

Similar to the cases of acyclic system,[3-5] depending on the molecular size of the cyclic pentacoordinate species, they either exist or do not exist as stable intermediates (the existence also depends on the bases sets used for the marginally stable intermediates). For example, a cyclic dianionic intermediate **2a**, which is formed by attack of OCH_3^{-} on ethylene phosphate monoanion (an analogue of RNA hydrolysis intermediate), can be located by ab initio calculations at the 3-21G* level.[1b] Although dianionic **2a** is only marginally stable at the 3-21G* level, a higher basis set such as 6-31+G* abolishes such an intermediate, which is similar to the results of Lim and Karplus for attack by OH^{-} on ethylene phosphate monoanion at the 3-21+G* calculation where there is only a pentacoordinate transition state (Figure 2A).[2] These results can be taken as an evidence to conclude that a pentacoordinate oxyphosphorane intermediate does not exist along the reaction path to base-catalyzed RNA hydrolysis. Although our present results also suggest that the pentacoordinate dianionic intermediate **2a** does not have a meaningful lifetime in the gas phase (Figure 2B), our more recent calculations on monoanionic **2a** indicate that *monoanionic phosphoranes* are much more stable in the gas phase (Figure 2C).[13] Taken all together, the absence of the dianionic intermediate **2b** (Lim and Karplus) and **3b** (this study) reveals that in these cases two negative charges cannot be delocalized over the small molecules at least in the gas phase; therefore, the intermediates do not exist. A slightly larger molecule of dianionic intermediate **2a** is the borderline case, and molecules of even larger sizes start to have a lifetime, although **2a** is still too short to really exist as a dianionic intermediate (Figure 2B), whereas a less charged monoanionic **2a** exists as a stable intermediate (which means that the well-depth is deep enough for monoanionic **2a** to have a meaningful lifetime).[13] Thus, it is expected that RNA hydrolysis intermediate **1** in the gas phase and hydrated **2a**[14] in alkaline solution exist as intermediates.

To generalize this conclusion, we also examined the solvent effect on the stability of a dianionic pentacoordinate intermediate: we carried out 3-21+G* level ab initio calculations for the water-solvated pentacoordinate dianionic oxyphosphorane **3b**, the simplest possible (least stable) model compound of this type. As we expected, the solvation of **3b** with water molecules allows dianionic **3b** to exist as a pentacoordinate intermediate on the potential surface.[14] These studies provide an overall picture as to when pentacoordinate intermediates exist and the nature of the transition states.

Methods of Calculations

All the calculations were carried out using the GAUSSIAN 86[15] and GAUSSIAN 90[16] programs on the following computers: FACOM M780/MSP, IBM 3090/MVS, IBM 6000/530 worksta-

(10) Sinnott, M. *Adv. Phys. Org. Chem.* **1988**, *24*, 113–204.
(11) Hine, J. *Adv. Phys. Org. Chem.* **1977**, *15*, 1–61.
(12) Uchimaru, T.; Storer, J. W.; Tsuzuki, S.; Tanabe, K.; Taira, K., submitted for publication.
(13) Uebayasi, M.; Uchimaru, T.; Taira, K. *Chem. Express* **1992**, *7*, 617–620.
(14) Yliniemela, A.; Uchimaru, T.; Tanabe, K.; Uebayasi, M.; Taira, K. *Nucleic Acids Res. Symp. Ser.* **1992**, *27*, 57–58. (b) Yliniemela, A.; Uchimaru, T.; Tanabe, K.; Taira, K. *J. Am. Chem. Soc.* **1993**, *115*, 3032–3033.

tion, or CRAY X-MP/216. The reaction profile for the base-catalyzed methanolysis of ethylene phosphate (right to left in Figure 4) was explored starting from the previously determined geometry of the stable pentacoordinate intermediate.[1b] The distances between P and $O_{(2)}/O_{(5)}$ were employed as the reaction coordinates. Points comprising the reaction profile were obtained through the geometry optimization at each value of the reaction coordinate without any additional constraint. The stationary points were fully optimized at the Hartree–Fock (HF) level of theory by using the analytical gradient technique,[17] and then vibrational frequencies were calculated by a normal coordinate analysis on force constants determined analytically. The thermodynamic parameters were calculated for the fully optimized structures of the stationary points on the potential energy surface of Figure 4 and the corresponding profile for the acyclic counterpart. The entropy and enthalpy changes between two states are given by the following equations.

$$\Delta S = \Delta S_{trans} + \Delta S_{rot} + \Delta S_{vib}$$

$$\Delta H = \Delta E + \Delta E_{trans} + \Delta E_{rot} + \Delta E_{vib} + P\Delta V$$

$$\Delta G = \Delta H - T\Delta S$$

In the present study, the energy surfaces were explored with the 3-21G* basis set, a split-valence basis set that includes d-functions (polarization functions) on phosphorus.[18,19] Although several computational studies suggest that minimal basis sets provide intrinsically similar stereoelectronic trends as do larger basis sets,[12,20,21] a larger basis set would provide more accurate geometries. Collins et al. compared the geometries and energies obtained by calculations at the STO-3G, 4-31G, and STO-3G* levels with the experimentally derived values.[22] It was concluded that the calculations at the STO-3G* provide the best electronic representation of hypervalent phosphorus and sulfur molecules. Similar comparison was made by Pietro et al. with respect to the still higher-level basis sets: 3-21G, 3-21G*, and 6-31G*.[18] The 3-21G* basis set gave almost the same molecular properties as the larger 6-31G* basis set. Similar trends were observed by Lowe et al. in an ab initio basis set study on hypervalent sulfur.[21] The agreement between the experimental values and 3-21G* geometries was excellent. In an ab initio study of negatively charged hypervalent phosphorus molecules, Streitwieser et al. suggested that the d-functions, particularly on phosphorus, are necessary for effective polarization stabilization of the anionic charge.[23] The conclusion is that d-functions on a hypervalent second-row atom are essential. It is also widely accepted that incorporation of diffuse functions would be important for representation of anionic species such as our model compounds **2** and **3**.[24,25] However, Lim and Karplus reported that calculations with the 3-21G* and 3-21+G* basis sets on the cyclic oxyphosphorane **2b** provide essentially the same reaction profile.[2] In the present study, we utilized the 3-21G* basis set for calculating reaction profiles for **2a**. However, to characterize the intermediate for **2a**, a 6-31G* calculation was also attempted. With respect to the simpler oxyphosphorane **3b** and hydrogen phosphate monoanion, we carried out higher level calculations (including 6-31+G*) as well. There was essentially no indication that the 3-21G* profile would be altered by higher computational levels (see ref 4 and the caption of Figure 5). Hence, we conclude that it would be safe to compare the characteristic features of the phosphorus diester bond cleavage processes in RNA analogues based on the 3-21G* reaction profiles. A higher basis set 6-31+G* also supports the nonexistence of the dianionic intermediate **3b**.

We also tested the effects of one and two water molecules on the stability of the pentacoordinate intermediate **3b**. The presence of one or two water molecules modified the potential surface to a remarkable extent, but no intermediate was found even after an extensive search. Thus, we decided to increase the number of water molecules immediately from two to six, which is the practical limit of our computational resources (optimization of **3b** with six water molecules took approximately 1 month of CPU time on an IBM 6000/530 workstation). The minimum number of water molecules needed to support the existence of the pentacoordinate intermediate **3b** is unknown.

Transition states *TS1* and *TS2* were located at the 3-21G* level and verified by frequency analysis to have only one imaginary frequency in the direction of reactants/products and the intermediate **2a**. The optimized parameters for *TS1*, **2a**, and *TS2* are presented in Figure 3. The conformational potential energy surface of **3b** was calculated with rigid rotamer approximation by using 30° grid and the geometrical parameters optimized for (*g*,*g*)-conformer (see Figure 5). The 3-D representation of the energy surface given in Figure 5 was obtained by means of SOLM0R in NUMPAC (Computer Center of Nagoya University).

The *TS1* structure was very close to the intermediate **2a**. *TS1* was located only after modification of the default step size and repeated evaluation of the Hessian. Due to the small step size and need for good second derivatives, *TS1* and *TS2* at 3-21G* calculations required the expenditure to over 100 h of CRAY X-MP CPU time to converge.

Results and Discussion

Model Reaction for Base-Catalyzed RNA Hydrolysis (Base-Catalyzed Methanolysis of Ethylene Phosphate, in a Reversed Direction). The reaction profile for $^-O(CH_2)_2OP(OCH_3)O_2^- \rightarrow (CH_2O)_2PO_2^- + OCH_3^-$ at the 3-21G* level is shown in Figure 4. This represents the attack of the RNA backbone by 2′-alkoxide followed by the expulsion of 5′-alkoxide via a pentacoordinate intermediate 1 (base-catalyzed RNA hydrolysis).[1] Structures at the stationary points are shown in Figure 3.

The stationary points representing the phosphorane intermediate **2a** (Figure 3b, and two transition state structures *TS1* (Figure 3a) and *TS2* (Figure 3c) can be described as minimally distorted trignal bipyramids (tbp). Although the normal 90° axial/equatorial bond angle in a tbp is slightly reduced to 80–89° for the ring $\angle O_{(2)}PO_{(3)}$ angle, accompanying a slight increase in non-ring-forming axial/equatorial bond angles such as $\angle O_{(2)}PO_{(equatorial)}$, the distortion does not originate from the constraints imposed by the five-membered $-PO_{(2)}CCO_{(3)}-$ring. The constraint-free $O_{(3)}PO_{(5)}$ angle also deviates from the normal 90° bond angle to the values ranging from 74 to 86° (Figure 3). One possible cause for the deviation is a negative charge repulsion between the axial $O_{(2)}/O_{(5)}$ and the most negatively charged equatorial oxygens. If the charge repulsion is indeed the main driving force of the deviation from tbp, even a greater deviation would be anticipated from an STO-3G optimized structure, since the STO-3G minimal basis set tends to exaggerate charge separation for hypervalent molecules. However, STO-3G structures resulted in a deviation of a similar magnitude,[1a] indicating that the charge repulsion is not the main cause for the deviation. Natural bond orbital (NBO) analysis[12] on **3b**,

(15) Frish, M. J.; Binkley, J. S.; Schlegel, H. B.; Raghavachari, K.; Melius, C. F.; Martin, R. L.; Stewart, J. J. P.; Bobrowicz, F. W.; Rohlfing, C. M.; Kahn, L. R.; Defrees, D. J.; Seeger, R.; Whiteside, R. A.; Fox, D. J.; Fleuder, E. M.; Pople, J. A. Carnegie-Mellon Quantum Chemistry Publishing Unit, Pittsburgh, PA, 1984.
(16) Frish, M. J.; Head-Gordon, M.; Trucks, G. W.; Foresman, J. B.; Schlegel, H. B.; Raghavachari, K.; Robb, M. A.; Binkley, J. S.; Gonzalez, C.; Defrees, D. J.; Fox, D. J.; Whiteside, R. A.; Seeger, R.; Melius, C. F.; Baker, J.; Martin, R. L.; Kahn, L. R.; Stewart, J. J. P.; Topiol. S.; Pople, J. A. Gaussian Inc., Pittsburgh, PA, 1990.
(17) Schlegel, H. B. *J. Comput. Chem.* **1982**, *3*, 214–218.
(18) Pietro, W. J.; Francl, M. M.; Hehre, W. J.; DeFrees, D. J.; Pople, J. A.; Binkley, J. S. *J. Am. Chem. Soc.* **1982**, *104*, 5039–5048.
(19) Dobbs, K. D.; Hehre, W. J. *J. Comput. Chem.* **1986**, *7*, 359–378.
(20) Lehn, J.-M.; Wipff, G. *J. Chem. Soc., Chem. Commun.* **1975**, 800–802.
(21) Lowe, G.; Thatcher, G. R. J.; Turner, J. C. G.; Waller, A.; Watkin, D. J. *J. Am. Chem. Soc.* **1988**, *110*, 8512–8520.
(22) Collins, J. B.; Schleyer, P. v. R.; Binkley, J. S.; Pople, J. A. *J. Chem. Phys.* **1976**, *64*, 5142–5151.
(23) Streitwieser, A., Jr.; Rajca, A.; McDowell, R. S.; Glaser, R. *J. Am. Chem. Soc.* **1987**, *109*, 4184–4188.
(24) Clark, T.; Chandrashekhar, J.; Spitznagel, G. W.; Schleyer, P. v. R. *J. Comput. Chem.* **1983**, *4*, 294–301.
(25) Spitznagel, G. W.; Clark, T.; Schleyer, P. v. R.; Hehre, W. J. *J. Comput. Chem.* **1987**, *8*, 1109–1116.

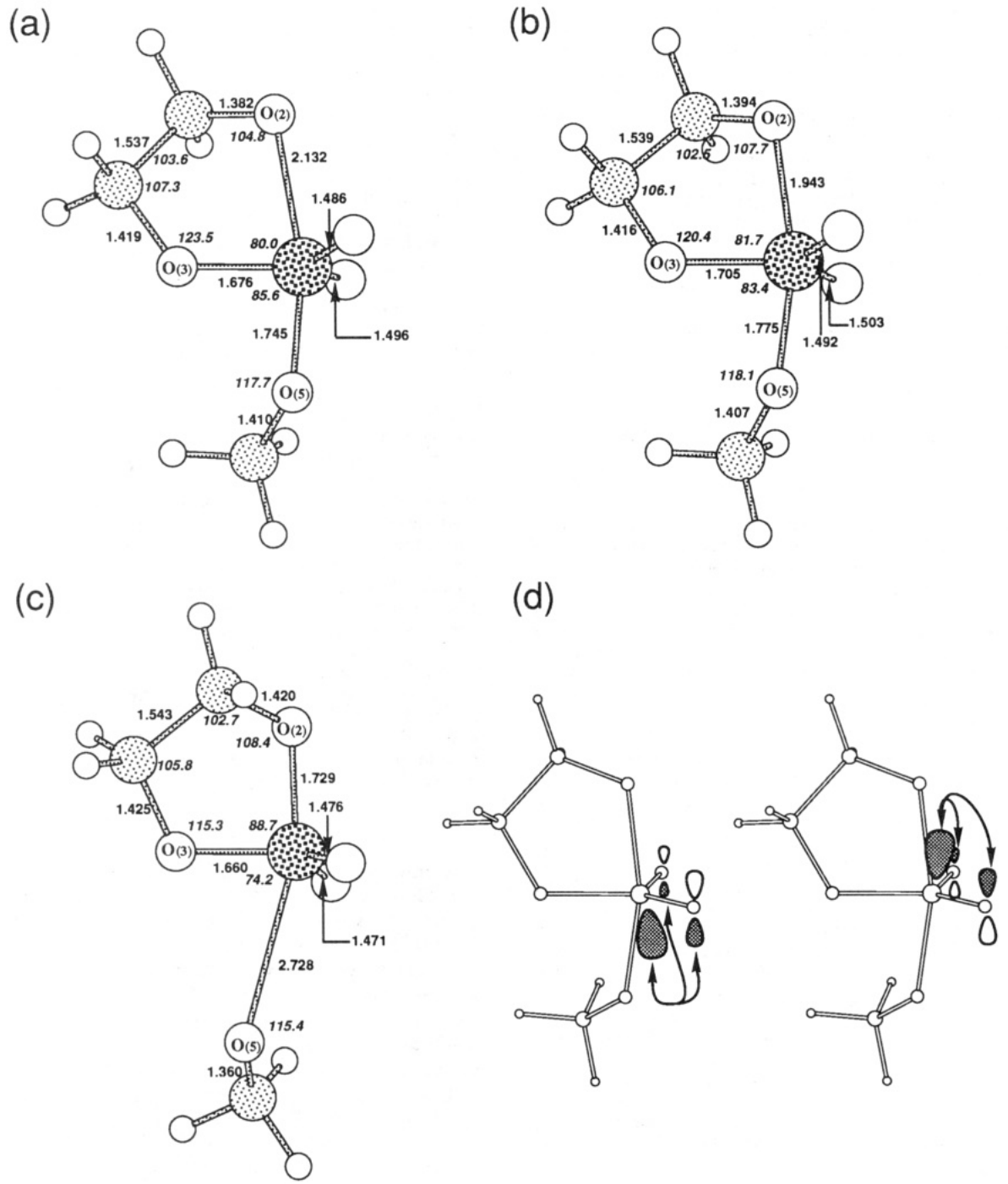

Figure 3. 3-21G*-optimized structures of the stationary points along the reaction path for $^{-}O(CH_2)_2OP(OCH_3)O_2^{-} \rightarrow (CH_2O)_2PO_2^{-} + OCH_3^{-}$: (a) the stereoelectronically favorable transition state (*TS1*) for endocyclic P–$O_{(2)}$ bond-forming step; (b) dianionic pentacoordinate intermediate **2a**; and (c) the stereoelectronically unfavorable transition state (*TS2*) for the exocyclic P–$O_{(5)}$ bond-breaking step. The optimized interatomic distances (Å) and interatomic angles (deg) are given in roman and in italic type, respectively. The imaginary frequencies for *TS1* and *TS2* are 155.4*i* and 115.4*i* cm^{-1}; (d) interactions between P–$O_{(2)/(5)}$ antibonding orbitals and lone-pair electrons on dianionic phosphoryl oxygens.

instead, indicates that the deviation is caused by the favorable orbital interactions between lone-pair electrons on the negatively charged phosphoryl oxygens ($O_{equatorial}$) and the antibonding orbitals of P–$O_{(2)}$/$O_{(5)}$ bonds. These interactions are schematically depicted in Figure 3d. These are pertinent to the idea that the n_{O3}–σ^*_{P-O2} orbital mixing interaction is not the structural determinant in the transition states.

The RHF/3-21G* activation energy leading to the first transition state *TS1* is 33.1 kcal/mol, and the barrier for the reversed reaction, i.e., for the attack by OCH_3^- on ethylene phosphate monoanion leading to the second transition state *TS2*, is 81.7 kcal/mol (Figure 4). The transition state *TS1* for breaking the endocyclic P–$O_{(2)}$ bond is only 0.24 kcal/mol above the putative intermediate **2a**. The *TS2* transition state is 13.8 kcal/mol above the intermediate. We also find that the endocyclic P–$O_{(2)}$ bond remains weaker than the exocyclic P–$O_{(5)}$ bond by 13.6 kcal/mol. Both 3-21G* and STO-3G[1] basis sets predict the weakened P–$O_{(5)}$ bond in *TS2* to be similar at 2.73 and 2.81 Å, respectively. Moreover, even when the intermediate does not exist, as in the case of **2b**, the concerted transition state structure looks like *TS2* (Figure 2A).[4,5] Therefore, it is important to point out that in all cyclic systems examined (Figure 2), the actual transition state

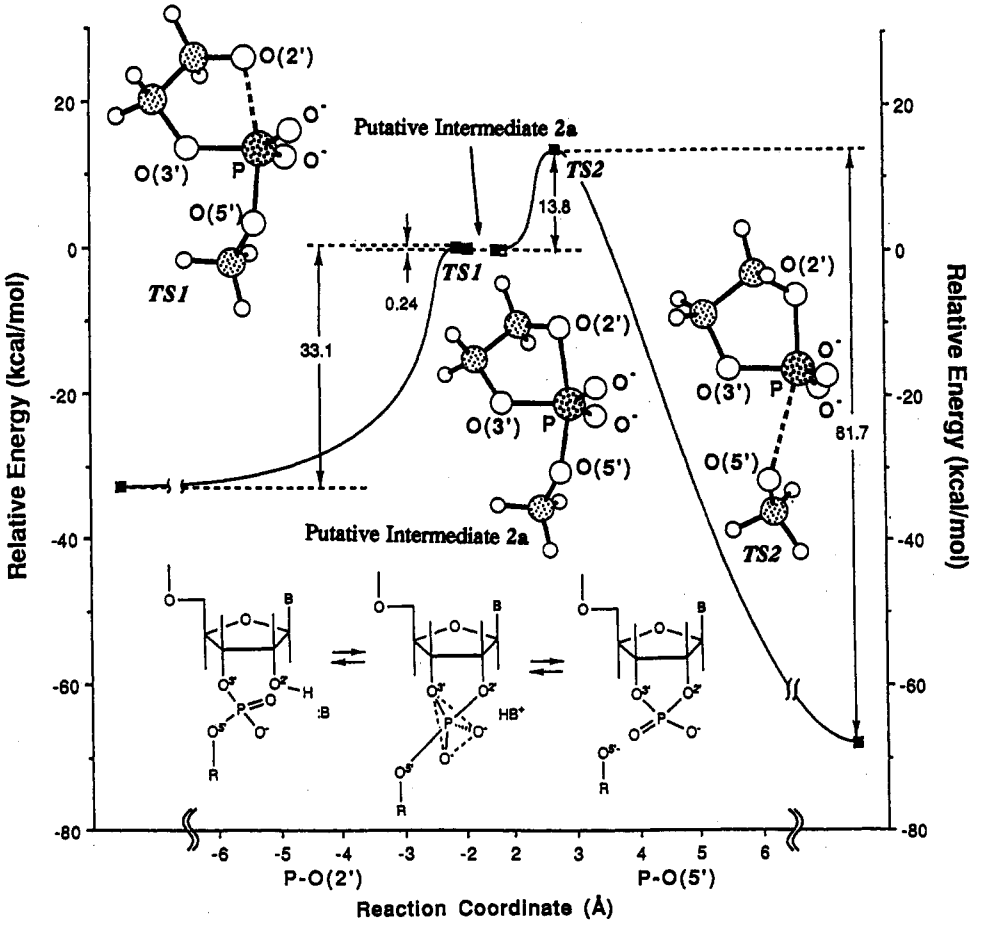

Figure 4. 3-21G* reaction profile for $^{-}O(CH_2)_2OP(OCH_3)O_2^{-} \rightarrow (CH_2O)_2PO_2^{-} + OCH_3^{-}$, modeling the base-catalyzed RNA hydrolysis. The vertical axis shows energy (kcal/mol) relative to the pentacoordinate intermediate **2a**. Numbers given inside figure represent potential energy differences (RHF energies).

Scheme I

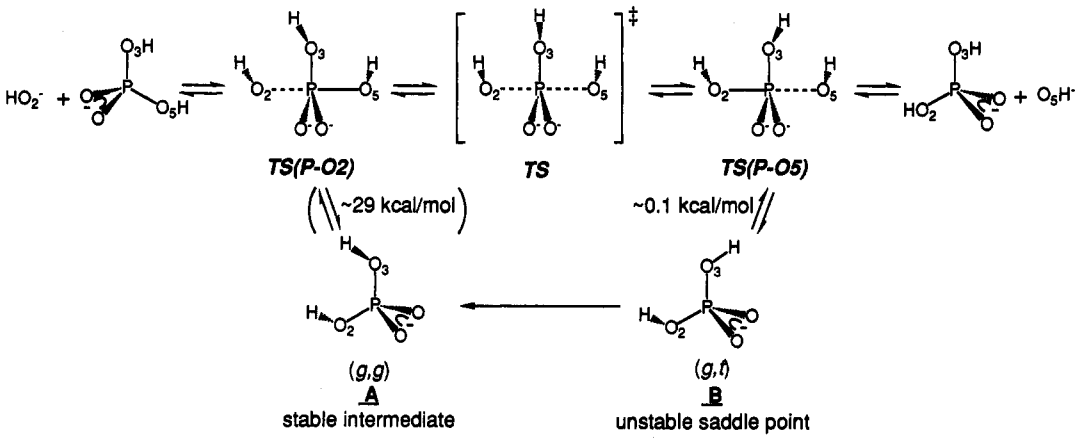

structure looks like *TS2* regardless of the lifetime of the pentacoordinate intermediate.

Energy Profiles for 2a and 3b Can Be Predicted from the Theory of Stereoelectronic Effect. The stereoelectronically unfavorable version of transition state *TS2* exists because of the unique cyclic nature of the intermediate (**1** or **2**). Alternatively, the acyclic counterparts such as **3a** and **3c**, having rotational freedom, cannot achieve the stereoelectronically unfavorable transition state.[3,5] Also, in the acyclic model reaction, the base-catalyzed hydrolysis of $H_2PO_4^{-}$ (i.e., $OH^{-} + (HO)_2PO_2^{-} \rightarrow$ **3b** $\rightarrow (HO)_2PO_2^{-} + OH^{-}$), at the 3-21G* level in C_s symmetry, the energy difference between the stereoelectronically favored and unfavored conformations about the equatorial P–$O_{(3)}$ bond is found to be 29 kcal/mol (Scheme I)[4]. Thus, the main energy difference between *TS1* and *TS2* in Figure 4 is not assigned to ring strain. In the case of **3b**, removal of the C_s symmetry constraint produces a transition state (see *TS* on Scheme I) rather than an intermediate at both 3-21G* and 3-21+G* levels (both levels yielded nearly identical results). At the transition state *TS*, the equatorial hydrogen atom on $O_{(3)}$ occupies the equatorial plane containing $O_{(3)}$ and two phosphoryl oxyanions. If this hydrogen atom on $O_{(3)}$ is tilted even a few degrees toward $O_{(2)}H$ as depicted in *TS*(P–O2), the *TS* starts to decompose and it is the P–$O_{(2)}$ bond which selectively undergoes cleavage. On the other hand, if the hydrogen atom is tilted toward $O_{(5)}H$ as in *TS*(P–O5), the P–$O_{(5)}$ bond-breaking proceeds. Thus, the shape of the potential energy surface is very sensitive to the orientation

of the equatorial $O_{(3)}$–H bond. Therefore, the mode of cleavage appears to be controlled primarily by the orientation of the lone pairs on $O_{(3)}$.

Note that in both *TS*(P–O2) and *TS*(P–O5) the lone pair electrons on $O_{(3)}$ are trans antiperiplanar to the breaking/forming bond. We call this reactivity dependence on the orientation of lone paired electrons a "stereoelectronic effect",[6-8] although we do not know the exact origin of the effect as to whether it is originated from orbital mixing, electrostatic, or dipolar interactions. Overlap populations and Mulliken charges are not necessarily in accord with the n_{O3}–σ^*_{P-O2} orbital mixing interpretation. Suggesting that the interpretation of the stereoelectronic effect only in terms of n_{O3}–$\sigma^*_{P-O(axial)}$ is questionable. We refer to "stereoelectronic effect" simply to indicate a reactivity dependence on the orientation of the equatorial P–O bond.

Can the Stereoelectronic Effect Be Explained by the Principle of Least Nuclear Motion? The exact origin of the stereoelectronic effects remains obscure. It is proposed that, in many cases, stereoelectronic interpretations can be rationalized by the principle of least nuclear motion (PLNM).[9-11] However, the interpretation of the reaction path given in Scheme I by means of the principle of least nuclear motion (PLNM) is difficult. According to PLNM, those elementary reactions will be favored that involve least change in atomic positions. And the effect of PLNM must be discernible when the transition state is a symmetrical one because, for reactions of an early transitions tate, the nuclear motions are small and the effect is negligible. Since the reaction in Scheme I proceeds via a symmetrical transition state, *TS*, it is a good system to test PLNM if the stereoelectronic prediction is different from the PLNM prediction.

Indeed, they predict different results. Consider the P–$O_{(5)}$ bond-breaking pathway. When we compare the stability of the end products, conformer **A** in the (*g*,*g*)-form is more stable than **B** (Scheme I). In fact, **B**, in the (*g*,*t*)-conformation does not exist as a stable intermediate, it is a saddle point as depicted in Figure 5. Thus, the consequence of P–$O_{(5)}$ bond breaking is **A**, where the $O_{(3)}$-hydrogen is gauche to the $O_{(2)}$ and hence the lone pair electrons on $O_{(3)}$ are partially trans antiperiplanar to the P–$O_{(2)}$H bond. Therefore, in order to minimize the nuclear motion, the $O_{(3)}$-hydrogen must stay facing toward $O_{(2)}$ when the P–$O_{(5)}$ bond is being broken, so that the most stable **A** with the (*g*,*g*) conformation can directly be produced via *TS*(P–O2) ($HO_{(2)}^-$ addition to phosphate → *TS*(P–O2) → **A**).

However, this is not a probable sequence of events; instead, the $O_{(3)}$-hydrogen rotates toward $O_{(5)}$ when the P–$O_{(5)}$ bond is being broken and it rotates toward $O_{(2)}$ when the P–$O_{(2)}$ bond is being broken. Thus, with PLNM, it is not easy to rationalize why the process of *TS* → *TS*(P–O2) → **A** does not take place; this process requires about 29 kcal/mol. In contrast, the other pathway accompanying double rotations of $O_{(3)}$-hydrogen (*TS* → *TS*(P–O5) → **B** → **A**) is energetically much more favorable, requiring only about 0.1 kcal/mol under C_s symmetry constraint.[4] Although at both *TS*(P–O2) and *TS*(P–O5) the $O_{(3)}$-hydrogen may stabilize the respective leaving hydroxide and this fact may be taken as the driving force to determine the mode of cleavage, similar behavior is observed when the $O_{(3)}$-hydrogen is replaced by an $O_{(3)}$-methyl group, which minimizes the stabilization of the leaving group by hydrogen bonding with the $O_{(3)}$-proton.[3]

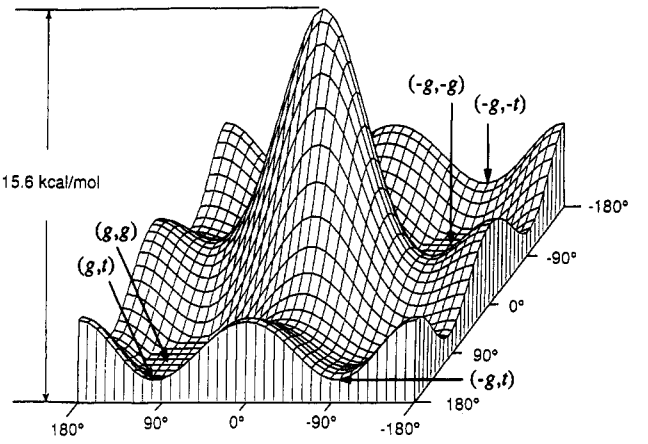

Figure 5. 3-D representation of 3-21G* conformational potential energy surface of hydrogen phosphate monoanion (**A** and **B** in Scheme I) as a function of two torsional angles about O–P–O–H. The energy surface was calculated with a rigid rotamer approximation by using a 30° grid and the geometrical parameters optimized for the (*g*,*g*)-conformer. The energy surface shows that the (*g*,*g*)-(conformer **A** in Scheme I) and (*g*,–*g*)-conformers are potential minima, whereas the (*g*,*t*)-conformer (conformer **B** in Scheme I) is a saddle point. In addition, the rigid rotamer approximation indicated that the (*g*,*g*)-conformer was preferred over the (*g*,–*g*)-conformer. These results were verified by complete geometry optimizations. The 3-21G* total energies (au) of completely optimized geometries are –638.223 77, –638.221 61, and –638.220 81, respectively, for the (*g*,*g*)- and (*g*,–*g*)-minima and the (*g*,*t*)-saddle point. The (*g*,*t*)-conformer has only one imaginary frequency (202.3*i* cm^{-1}) corresponding to P–O bond rotation. With respect to the (*g*,*g*)-minimum, geometry optimization was carried out at the 3-21+G* and 6-31+G* levels as well. The total energies (au) of 3-21+G* and 6-31+G* minima are –638.349 57 and –641.499 07, respectively. The O–P–O–H torsional angle for the (*g*,*g*)-minimum is calculated to be 107.0°, 98.4°, and 96.1°, respectively, at the 3-21G*, 3-21+G*, and 6-31+G* levels.

Clearly, stereoelectronic arguments have better predictive power than PLNM in these gas-phase reactions. Recently, King and Rathore have examined the geometry-dependent substituent effect on the rate of H–D exchange in cyclic sulfones by using NMR techniques.[26] Pertinent to our findings, their results provide a solution-phase example of a kinetic anomeric effect not readily accounted for by PLNM. However, alternatively, a stereoelectronic effect in the gas phase may originate from the electrostatic or bond dipole interactions rather than n–σ^* orbital mixing.[12]

Existence of Dianionic Pentacoordinate Intermediates (Theory and Experiment). Regarding the stability of pentacoordinate dianionic intermediates, those such as **2b** and **3b** with small substituents appear less stable and exist only as transition states. Bigger substituents better delocalize the dianionic charges and stabilize the intermediates in the gas phase (see Table I and Figure 2).[27] The alkyl groups on oxygens reduce the negative charges at phosphorus and oxygen atoms. The total charge of the PO_5 moiety of **3a** is –2.663, which is appreciably decreased from the value of –3.520 for **3b**, by substitution of the hydrogens with methyl groups (Table I). In that sense, an RNA intermediate **1** is expected to be more stable than **2**. As shown in Figure 4, dianionic intermediate **2a** is the borderline case and is only marginally stable at 3-21G* level. Further, when zero-point energy is included, the dianionic intermediate **2a** on the potential surface

(26) King, J. F.; Rathore, R. *J. Am. Chem. Soc.* **1990**, *112*, 2001–2002.
(27) See the next section as well.

Table I. NBO Charges for Oxyphosphoranes[a]

	3a(TS)[b]	3b(TS)[c]	3b + $6H_2O$[d]	3b (monoanion)[e]
P	2.713	2.689	2.738	2.712
O_2	−0.927	−1.167	−1.140	−1.150
O_3	−0.926	−1.120	−1.093	−1.099
O_5	−0.927	−1.167	−1.190	−1.149
Oeq1	−1.285	−1.310	−1.292	−1.099
Oeq2	−1.311	−1.344	−1.323	−1.288
sum	−2.663	−3.520	−3.300	−3.074
H_2 (CH_3)	0.191	0.463	0.507	0.506
H_3 (CH_3)	0.281	0.494	0.534	0.531
H_5 (CH_3)	0.191	0.463	0.505	0.506
$H_{eq}1$				0.531
sum	−2.000	−2.000	−1.755	−1.000

[a] NBO charges were calculated at the 3-2+G* level. [b] Dianionic oxyphosphorane **3a** transition state. [c] Dianionic oxyphosphorane **3b** transition state. [d] Dianionic oxsyphosphorane **3b** intermediate solvated with six water molecules. [e] Monoanionic oxyphosphorane **3b** intermediate.

Table II. Calculated Thermodynamic Parameters[a-c]

cyclic 2a		acyclic 3a[d]	
$\Delta G^{\ddagger}$(MHEP[e] → TS1)	32.3		
$\Delta H^{\ddagger}$(MHEP → TS1)	31.8		
$\Delta S^{\ddagger}$(MHEP → TS1)	−1.9		
$\Delta G^{\ddagger}$(2a → TS1)	−0.19	$\Delta G^{\ddagger}$(3a → TS)	−0.027
$\Delta H^{\ddagger}$(2a → TS1)	−0.50	$\Delta H^{\ddagger}$(3a → TS)	0.39
$\Delta S^{\ddagger}$(2a → TS1)	−1.1	$\Delta S^{\ddagger}$(3a → TS)	1.4
$\Delta G^{\ddagger}$(2a → TS2)	10.0		
$\Delta H^{\ddagger}$(2a → TS2)	11.9		
$\Delta S^{\ddagger}$(2a → TS2)	6.4		
$\Delta G^{\ddagger}$(EP + MeO^- → TS2)	93.4	$\Delta G^{\ddagger}$(DMP[e] + MeO^- → TS)	91.7
$\Delta H^{\ddagger}$(EP + MeO^- → TS2)	82.0	$\Delta H^{\ddagger}$(DMP + MeO^- → TS)	79.1
$\Delta S^{\ddagger}$(EP + MeO^- → TS2)	−38.3	$\Delta S^{\ddagger}$(DMP + MeO^- → TS)	−42.2
		$\Delta G^{\ddagger}$(3a → RTS)	1.98
		$\Delta H^{\ddagger}$(3a → RTS)	1.02
		$\Delta S^{\ddagger}$(3a → RTS)	−3.2

[a] Calculated at 3-21G* level at 298.15 K. [b] Unit for $\Delta G^{\ddagger}$ and $\Delta H^{\ddagger}$ is kcal/mol and unit for $\Delta S^{\ddagger}$ is eu (cal/mol·K). [c] Abbreviations: MHEP, methyl hydroxyethyl phosphate dianion; EP, ethylene phosphate monoanion; DMP, dimethyl phosphate monoanion; TS, transition state for axial P–O bond forming/breaking step; RTS, rotational transition state (see ref 3). Total energies (au) and zero-point energies (kcal/mol in the parentheses) are as follows. MHEP, −828.353 04 (77.24); TS1, −828.300 30 (76.18); **2a**, −828.300 69 (76.67); TS2, −828.278 78 (74.57); EP, −714.684 18 (50.46); MeO^-, −113.724 80 (23.67); **3a**, −829.450 12 (89.77); TS −829.447 97 (88.95); DMP((*g*,*g*)-conformer); −715.847 78 (63.77); RTS, −829.447 30 (89.42). [d] The calculated thermodynamic parameters for pentacoordinate oxyphosphorane intermediate/transition state with two axial methyl groups occupying trans regions of the equatorial ester P–$O_{(3)}$ bond. See refs 3 and 12 for more details. [e] Thermodynamic parameters were calculated with respect to the most stable conformer.

disappears (Table II); the zero-point energy is 76.67 kcal/mol for the intermediate **2a** relative to 76.18 kcal/mol for the endocyclic cleavage transition state *TS1* [note that the numbers given in Figure 4 represent potential energies (3-21G* RHF energies) and those given in Table II are ΔG, ΔH, and ΔS in which frequencies are not scaled]. In agreement with this lower stability, the dianionic intermediate **2a** disappears from the potential energy surface at the 6-31+G* level.

The dianionic intermediate, however, is expected to be more stabilized by solvation relative to two monoanionic reactants. The dipole moment of the 3-21G* optimized intermediate **2a** (6.885 D) is slightly greater in value than the 3-21G* optimized transition state *TS1* (6.675 D); thus, the intermediate is more favorably stabilized than the transition state upon solvation. The ionic state also has a strong influence on the lifetime of the intermediate;

Scheme II

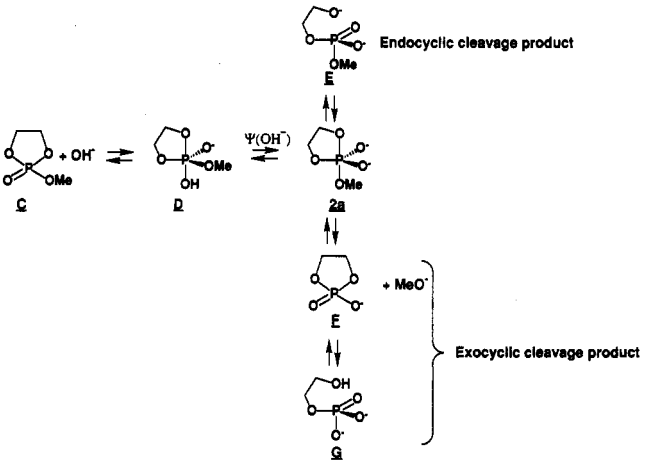

although *TS1* for the dianionic intermediate **2a** is only 0.24 kcal/mol above the intermediate, the corresponding value for the monoanionic **2a** is 3.5 kcal/mol at 3-21G* level (the activation barrier from the intermediate to *TS2* is almost unaffected; 15.5 kcal/mol); thus, the monoanionic intermediate is more stable.[13] The instability of the dianionic pentacoordinate intermediate in the gas phase is caused by the lack of delocalization of the two negative charges by means of, e.g., large substituents and/or more importantly by solvation. In accord with this interpretation, even the smallest (least stable in gas phase) dianionic **3b** species appears to exist as a stable intermediate under hydrated conditions as we will discuss in the last section.

Experimental results show that the dianionic intermediate **2a** *does exist* since, as depicted in Scheme II, the hydrolysis of methyl ethylene phosphate **C**[28-30] in 5 M NaOH yields 2–4% exocyclic product **G**, via **F**.[31] In the initial step of the reaction, hydroxide attacks on **C** from the axial position yielding **D**. Then, since the departure of methoxide can take place only from the axial position of **2a**[4] giving rise to 2–4% exocyclic cleavage product **G**, a pseudorotation[32] of the initial intermediate (**D** → **2a**) is mandatory: without the formation of initial intermediate **D**, no pseudorotation and thus no **2a**/exocyclic products (**F** and **G**) would be expected. This experimental observation (the existence of 2–4% exocyclic product **G**) provides strong evidence for the existence of dianionic pentacoordinate intermediate **2a** in alkaline solution. Therefore, solvation apparently stabilizes the dianionic intermediates (see the last section for the detailed discussion).

Discrepancy between Solution- and Gas-Phase Potential Energy Surfaces. According to Figure 4, no exocyclic cleavage should take place since *TS2* is 13.6 kcal/mol higher in energy than *TS1* (see also thermodynamic parameters in Table II). However, this expectation is defied by experiment as discussed in the previous section: in 5 M NaOH, exocyclic products were identified.[28-31] The presence of 2–4% exocyclic product indicates that the energy difference between *TS1* and *TS2* in alkaline solution is at most ~2 kcal/mol since parts of the

(28) Kluger, R.; Covitz, F.; Dennis, E. A.; Williams, D.; Westheimer, F. H. *J. Am. Chem. Soc.* **1969**, *91*, 6066–6072.
(29) Kluger, R.; Thatcher, G. R. J. *J. Am. Chem. Soc.* **1985**, *107*, 6006–6011.
(30) Kluger, R.; Thatcher, G. R. J. *J. Org. Chem.* **1986**, *51*, 207–212.
(31) Gorenstein, D. G.; Chang, A.; Yang, J.-C. *Tetrahedron* **1987**, *43*, 469–478.
(32) Westheimer, F. H. *Acc. Chem. Res.* **1968**, *1*, 70–78.

endocyclic product **E** could originate directly from **D** rather than **2a**. This kind of discrepancy between the theoretical gas-phase calculations and the solution experiments challenges the stereoelectronic arguments.[10,33,34] It is also necessary to point out that, despite the well-known enhanced reactivity of five-membered cyclic phosphate esters in aqueous solution, the calculated gas-phase thermodynamic parameters ($\Delta H^{\ddagger}$) for cyclic (**2a**) and acyclic (**3a**) compounds failed to reproduce the reactivity difference (Table II).[33] Solvation apparently modifies the potential energy surface for this reaction. Differences also exist between cyclic and acyclic entropies of activation. However, considering the conformational freedom of dimethyl phosphate monoanion (DMP) (see Figure 5 of four possible conformers for an acyclic compound, whereas only one conformer is possible for cyclic ethylene phosphate monoanion), the actual $\Delta G^{\ddagger}$(DMP + MeO^- → TS) is expected to increase to a larger value than that given in Table II because a larger $\Delta S^{\ddagger}$(DMP + MeO^- → TS) would result, making the acyclic compound less reactive than the expectation based on the $\Delta G^{\ddagger}$(DMP + MeO^- → TS) value.

Meanwhile, an examination of intrinsic reactivity differences is an important first step to study gas-phase reactions: note, for example, that the solution-phase acidity/basicity involving solvation became clearer after the gas-phase intrinsic acidity/basicity of reversed order had been recognized. Before the advent of gas-phase experimental measurements, the observation in solution that substituting one hydrogen of H_2O by successively more bulky alkyl groups causes a steady lowering of acidity was generally interpreted in terms of the inductive effects of the alkyl groups. It was presumed that an alkyl group, being evidently electron-donating group since it stabilizes carbocation, should destabilize a negative charge. Thus, an alcohol like $(CH_3)_3COH$ should have less tendency to form a negative ion by loss of a proton and hence should be least acidic ($(CH_3)_3CO^-$ being the strongest base). However, the gas-phase measurements showed that, in the absence of solvent, water is the weakest acid (OH^- being the strongest base) and $(CH_3)_3COH$ is the strongest acid ($(CH_3)_3CO^-$ being the weakest base).[35] Therefore, the solution data (the inductive effects) has been misinterpreted in the past. Apparently, alkyl groups are better able to stabilize not only positive charge but also negative charge than is hydrogen as we also have indicated in the section of Existence of Dianionic Pentacoordinate Intermediates.

Pentacoordinate Oxyphosphorane Intermediates Always Exist Once They Have Been Sufficiently Solvated. During the acid-catalyzed hydrolysis of hydrogen ethylene phosphate and methyl ethylene phosphate (**C** in Scheme II) in ^{18}O-labeled water, the labeled oxygen can be incorporated into the unreacted ester.[28,36] In addition, significant phosphoryl migration from the 3′ to the 2′ hydroxyl group of the ribonucleotide takes place under acidic conditions.[37,38] These results suggest the existence of a pentacoordinate intermediate that can undergo pseudorotation in acidic media. By contrast, base-catalyzed hydrolysis is not accompanied by ^{18}O exchange,[36] and no phosphoryl migration is apparent.[37,38] In accord with the above-mentioned gas-phase calculations, the latter results can be rationalized by assuming the nonexistence of pentacoordinate intermediates in basic media.[2-5,13,14] However, as we discussed above, solvation significantly modifies the potential energy surface and as a result stabilizes dianionic pentacoordinate intermediates. We have thus chosen the least stable dianionic **3b** (Scheme I) which shows no indication of an intermediate and examined the change of the energy surface upon hydration. We carried out an intrinsic reaction coordinate (IRC) calculation, starting from the 6-31+G* transition state (Table III). The total energy of the pentacoordinate species decreased monotonously by 10.76 kcal/mol during the lengthening of the axial P–O bond from 1.859 to 2.002 Å. The full optimization starting from that point led right away to the elimination of the axial hydroxyl group. We therefore conclude that the pentacoordinate intermediate does not exist for dianionic **3b** along the gas-phase reaction profile.[14]

As we expected, the solvation of **3b** with water molecules allows dianionic **3b** to exist as the pentacoordinate intermediate on the potential surface. We tested the effects of one and two water molecules on the stability of the pentacoordinate intermediate **3b**.[14] The presence of water molecules modified the potential surface to a remarkable extent, but no intermediate was found even

Table III. Geometries of Transition States and the Water-Solvated Minimum Structure of Dianionic Oxyphosphorane (3b)[a]

	3b (TS)[b]		3b + $6H_2O$[c]
basis set	3-21+G*[d]	6-31+G*[e]	3-21+G*
P–O_2	1.842	1.859	1.735
P–O_3	1.692	1.689	1.642
P–O_5	1.842	1.859	1.818
P–Oeq1	1.524	1.508	1.544
P–Oeq2	1.547	1.527	1.570
H–O_2	0.965	0.946	0.965
H–O_3	0.965	0.947	0.964
H–O_5	0.965	0.946	0.963
Oeq2–P–O_3	112.9	112.8	126.5
Oeq1–P–O_3	111.5	112.3	118.6
O_5–P–O_3	87.4	87.3	81.9
O_2–P–O_3	87.4	87.3	84.0
H–O_5–P	106.9	102.2	114.2
H–O_2–P	106.9	102.2	113.7
H–O_3–P	110.0	104.0	109.7
Oeq1–P–O_3–Oeq2	180.0	180.0	−175.8
O_5–P–O_3–Oeq2	−88.7	−89.1	−85.0
O_2–P–O_3–Oeq2	88.7	89.1	89.0
H–O_5–P–O_3	98.2	95.4	146.8
H–O_2–P–O_3	−98.2	−95.4	−160.7
H–O_3–P–Oeq2	180.0	180.0	87.8
E(RHF)[f]	−713.198 07	−716.713 91	−1167.186 63

[a] Internal coordinates are given in Å and deg. [b] Dianionic oxyphosphorane **3b** transition state. [c] Dianionic oxyphosphorane **3b** intermediate solvated with six water molecules. No imaginary frequency is found for fully optimized 3-21+G* structure. [d] Imaginary frequency: 455.7i cm^{-1}. [e] Imaginary frequency: 447.7i cm^{-1}. We carried out an intrinsic reaction coordinate (IRC) calculation, starting from the 6-31+G* transition state. The total energy of the pentacoordinate species decreased monotonously by 10.76 kcal/mol during the lengthening of the axial P–O bond from 1.859 to 2.002 Å. The full optimization starting from that point led right away to the elimination of the axial hydroxyl group. We therefore conclude that the pentacoordinate intermediate does not exist for dianionic **3b** along the gas-phase reaction profile. [f] Total energies are given in au.

(33) Kluger, R.; Taylor, S. D. *J. Am. Chem. Soc.* **1990**, *112*, 6669–6671.
(34) Thatcher, G. R. J.; Kluger, R. *Adv. Phys. Org. Chem.* **1989**, *25*, 99–265.
(35) Lowry, T. H.; Richardson, K. S. *Mechanism and Theory in Organic Chemistry*; Harper & Row: New York, 1976.
(36) Haake, P. C.; Westheimer, F. H. *J. Am. Chem. Soc.* **1961**, *83*, 1102–1109.
(37) Brown, D. M.; Usher, D. A. *Proc. Chem. Soc.* **1963**, 309–310.
(38) (a) Anslyn, E.; Breslow, R. *J. Am. Chem. Soc.* **1989**, *111*, 4473–4482. (b) Breslow, R.; Huang, D. L.; Anslyn, E. *Proc. Natl. Acad. Sci. U.S.A.* **1989**, *86*, 1746–1750.

(39) Optimization of **3b** with six water molecules took approximately 1 month of CPU time on an IBM 6000/530 workstation.

after an extensive search. Thus, we decided to increase the number of water molecules from two to six, which is the practical limit of our computational resources.[39] The minimum number of water molecules needed to support the existence of the pentacoordinate intermediate **3b** is unknown. The location of the solvated intermediate with six water molecules was carried out by two-step geometry optimizations. First, the solvated system was optimized under C_s symmetry constraints with respect to its equatorial plane. Next, starting from this C_s structure, full optimization was carried out without any symmetrical constraints at the 3-21+G* level. The frequency calculation ensured that the final structure had no imaginary frequencies. Thus, it is indeed a pentacoordinate intermediate (Figure 6).

The NBO analysis of water-solvated **3b** indicates that water solvation has a qualitatively similar effect to that of alkyl groups: it reduces the negative charge of **3b**, thus causing the dianionic compound to behave in a manner more characteristic of a stable monoanionic compound (Table I and Figure 2). The stability of the charged intermediate is, thus, greatly increased in the presence of water molecules by the delocalization of negative charges. The NBO charge of dianionic oxyphosphorane **3b**, when it is solvated with six water molecules, is reduced from −2.000 to −1.755. The water molecules accommodate part of the negative charges (Table I).

We have thus shown that even the least stable dianionic **3b** can exist, once it is sufficiently hydrated, as a stable pentacoordinate intermediate. Since naked dianionic **3b**, monohydrated **3b**, or dihydrated **3b** cannot exist as intermediates, the extent of hydration is, of course, important. Nevertheless, the results presented here led us safely to the conclusion that, in aqueous solution, when species are sufficiently hydrated, any pentacoordinate oxyphosphorane can exist as an intermediate. Thus, the lack of ^{18}O exchange and the lack of phosphoryl migration under basic conditions should be interpreted as a consequence of a high energy barrier to pseudorotation,[4,40] and such results should not be taken as evidence against a pentacoordinate intermediates. Solution-phase phosphoryl-transfer reactions can take place via a pentacoordinate oxyphosphorane intermediate not only under acidic but also under basic conditions.

Conclusion

We have analyzed the oxyphosphoranes listed in Figure 1 and provided an explanation as to why certain pentacoordinate species can exist as stable intermediates in the gas phase (Figure 2). Especially in a model reaction for base-catalyzed RNA hydrolysis, or in reverse, the attack of OCH_3^- on ethylene phosphate monoanion, a pentacoordinated dianionic intermediate **2a** has been shown to be the borderline case between the concerted reaction of dianionic **2b** (Figure 2A) and the stepwise reaction of monoanionic **2a** (Figure 2C). Moreover, we have shown that the least stable dianionic **3b** can exist, once it has been sufficiently hydrated, as a stable pentacoordinate intermediate (Figure 6). This analysis suggests that all oxyphosphoranes listed in Figure 1 and related compounds can exist as pentacoordinate intermediates once they have been sufficiently solvated.

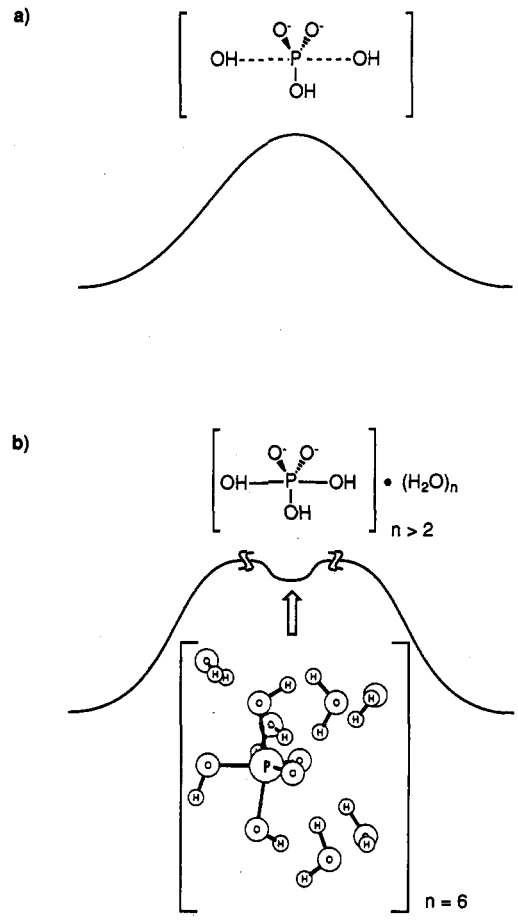

Figure 6. Schematic representations of reaction profiles for $OH^- + H_2PO_4^- \rightarrow [H_3PO_5^{2-}] \rightarrow H_2PO_4^- + OH^-$. (a) Ab initio calculations indicate that the pentacoordinate intermediate does not exist along the gas-phase reaction coordinate. Thus, the reaction takes place in a single-step mechanism in the gas phase. The activation energy of the reaction is calculated to be 92 kcal/mol at the 3-21+G* level (the total energies of OH^-, $H_2PO_4^-$, and $[H^3PO_5^{2-}]$ are −74.995 74, −638.349 57, and −713.198 07 au, respectively). (b) However, the present work shows that solvation with water molecules allows dianionic oxyphosphorane species to exist as the pentacoordinate intermediate. The optimized structure of **3b**, hydrated with six water molecules, is also depicted.

Acknowledgment. We thank Dr. Mutsumi Aoyagi of National Institute of Materials and Chemical Research for helpful comments and discussions. We also thank the Computer Center (RIPS) for a generous allocation of computing time.

(40) Wasada, H.; Hirao, K. *J. Am. Chem. Soc.* **1992**, *114*, 16–27.